

**Special Section:**

Fire in the Earth System

Key Points:

- Particulate matter and CO emission factors (EFs) are highly sensitive to the burning conditions of the fuel
- A correlation was found for CO and PM emissions generated by combustion of wood fuel in a tube furnace and measured in a laboratory chamber
- Fuel nitrogen content plays a significant role in the EF of NO

Supporting Information:

Supporting Information may be found in the online version of this article.

Correspondence to:

S. Bililign,
bililign@ncat.edu

Citation:

Pokhrel, R. P., Gordon, J., Fiddler, M. N., & Bililign, S. (2021). Determination of emission factors of pollutants from biomass burning of African fuels in laboratory measurements. *Journal of Geophysical Research: Atmospheres*, 126, e2021JD034731. <https://doi.org/10.1029/2021JD034731>

Received 7 FEB 2021

Accepted 5 OCT 2021

Author Contributions:

Conceptualization: Rudra P. Pokhrel, Marc N. Fiddler, Solomon Bililign

Data curation: Rudra P. Pokhrel

Formal analysis: Rudra P. Pokhrel

Funding acquisition: Solomon Bililign

Investigation: Rudra P. Pokhrel, Janica Gordon, Marc N. Fiddler

Methodology: Rudra P. Pokhrel, Janica Gordon

Project Administration: Solomon Bililign

© 2021. The Authors.

This is an open access article under the terms of the [Creative Commons Attribution License](#), which permits use, distribution and reproduction in any medium, provided the original work is properly cited.

Determination of Emission Factors of Pollutants From Biomass Burning of African Fuels in Laboratory Measurements

Rudra P. Pokhrel^{1,2,3} , Janica Gordon⁴, Marc N. Fiddler^{5,6} , and Solomon Bililign^{1,4,6} 

¹Department of Physics, North Carolina A&T State University Greensboro, NC, USA, ²Now at Cooperative Institute for Research in Environmental Sciences, University of Colorado, Boulder, CO, USA, ³Now at Chemical Sciences Laboratory, National Oceanic and Atmospheric Administration, Boulder, CO, USA, ⁴Department of Applied Sciences and Technology, North Carolina A&T State University, Greensboro, NC, USA, ⁵Department of Chemistry, North Carolina A&T State University, Greensboro, NC, USA, ⁶ISET Center North Carolina A&T State University, Greensboro, NC, USA

Abstract Biomass burning (BB) is a major source of pollutants that impact local, regional, and global climate, air quality, and public health. However, the influence of burning conditions and fuel type on the emission factors of pollutants is still not well understood. Here, we present the results from a laboratory study of emission factors (EFs) of pollutants from six different sub-Saharan African biomass fuels combusted under a wide range of burning conditions, ranging from smoldering to flaming. We found that particulate matter (PM) and carbon monoxide (CO) EFs (g (kg wood)^{-1}) are highly sensitive to the burning conditions, with an order of magnitude variation between flaming and smoldering burning conditions. Nitric oxide (NO) EF shows a fuel type dependence, with higher NO EFs for fuels with larger nitrogen content. While CO is not generally a proxy for $\text{PM}_{2.5}$ emissions, in this work a correlation was found between CO and PM emissions generated by combustion of seven wood fuels with moisture content (dry basis) <10% in a tube furnace and measured from a laboratory smog chamber with a temperature of $\sim 21\text{--}24^\circ\text{C}$ and an RH below 5%. Unlike total PM, EFs of inorganic particle-phase species do not show dependence on burning conditions. Finally, we showed that burning biomass fuels in a tube furnace would be a useful experimental approach to study BB emission under controlled burning conditions.

Plain Language Summary Biomass burning is a major source of pollutants that impact climate, air quality, and health. However, the influence of burning conditions and fuel type on the emission factors (EFs) of pollutants is not well understood. An EF relates the quantity of a pollutant released to the atmosphere for a given combustion process and is expressed as grams of emission per kilogram of fuel burned. EFs provide a means to estimate where and how much a pollutant is emitted from various sources so that air quality can be modeled. There are very limited measurements of EFs for African fuels. Here, we present the results from a laboratory study of emission factors of pollutants from six different sub-Saharan African wooden biomass fuels combusted under a wide range of burning conditions, ranging from smoldering to flaming. We found that the EF of particulate matter and carbon monoxide are sensitive to the burning condition and the EF of nitric oxide depends on the nitrogen content of the fuel. A possible correlation between carbon monoxide emission and particulate matter emission is observed. A tube furnace was used to generate the BB emissions in this work, which offered an opportunity to conduct controlled burning in the laboratory.

1. Introduction

Biomass burning (BB), which includes burning in open fires as well as in cookstoves (Akagi et al., 2011), emits gaseous and particulate pollutants that impact human health, including premature deaths and low birth weight. Emissions from BB are associated with a variety of acute respiratory illnesses such as asthma, chronic obstructive pulmonary disease, pulmonary fibrosis, pneumonia, and lung cancer (Delfino et al., 2009; Elliott et al., 2013; Henderson et al., 2011; Holstius et al., 2012; Johnston et al., 2011, 2012; Naehler et al., 2007; Rappold et al., 2011; Smith & Pillarisetti, 2017; Stefanidou et al., 2008; Sutherland et al., 2005). Air pollution (ambient and household) is a major threat to human health, which increases the

Software: Marc N. Fiddler
Supervision: Marc N. Fiddler, Solomon Bililign
Writing – original draft: Rudra P. Pokhrel
Writing – review & editing: Marc N. Fiddler, Solomon Bililign

risk of pulmonary and cardiovascular diseases and results in the annual premature death of an estimated 7 million people globally (Forouzanfar, 2016). BB is the largest source of primary carbonaceous particles and the second largest source of trace gases in the atmosphere (Andreae, 2019; Andreae & Merlet, 2001; Bond et al., 2004). The impacts of air pollution in Africa are significant, since Africa is the single largest source of BB emissions; accounting for more than half of global BB carbon emissions (Ichoku et al., 2008, 2016; Lamarque et al., 2010; Roberts et al., 2009; Roberts & Wooster, 2008; Schultz et al., 2008; van der Werf et al., 2010). Emissions from Africa are expected to grow due to a rapid increase in population. By 2100, the population of Africa is predicted to be 40% of the global population (UN, 2017). The sharp increase in population will increase the use of domestic and commercial combustion sources of energy, since it is estimated that about 500 million people will remain without access to electricity by 2030 (IEA, 2020). In 2018, about 900 million people in sub-Saharan Africa relied on solid fuel, and that demand is expected to grow sharply (IEA, 2020). Solid fuels such as wood, charcoal, animal dung, and crop residue are the main sources of energy in African households (Beyene & Koch, 2013). Besides health impacts, emissions from Africa will also impact the global climate. Black carbon (BC), which is second only to carbon dioxide (CO₂) in its climate warming contribution (Bond et al., 2013; Jacobson, 2001), is a main constituent in particulate matter emitted from BB. Up to 80% of the BC emissions from Africa were attributed to residential solid fuel burning (Bond et al., 2013).

Even though Africa is the largest source of global BB carbon emission, studies focusing on African BB emissions are recent and very limited (Eck et al., 2003; Flamant et al., 2018; Haywood et al., 2020; Redemann et al., 2020; Vakkari et al., 2014). Most of the global emission inventories available and used for Africa are based on emissions data from North America, Europe, and Asia (Bond et al., 2004, 2007; Klimont et al., 2009, 2013; Lamarque et al., 2010; Streets et al., 2004). The use of such inventories for air quality and climate modeling studies in Africa have resulted in large uncertainties (Assamoi & Liousse, 2010; Liousse et al., 2010, 2014). One way to reduce these uncertainties is to use emission factors (EFs) derived from local measurements of African fuels in the emission inventories. There have been several field studies reporting cookstove emissions in Africa (Adkins et al., 2010; Beltramo & Levine, 2013; Coffey et al., 2017; Eilenberg et al., 2018; Jary et al., 2014; Johnson et al., 2011; Oluwole et al., 2013; Pennise et al., 2009; Rosa et al., 2014; Wathore et al., 2017), but most of the studies are limited to only a few air pollutants; mostly CO and particulate matter (PM) (Thomas et al., 2015). Variabilities in estimated EFs are attributed to factors like stove type, fuel type, moisture content, fuel origin, etc. which makes direct comparison of the results difficult. Due to a lack of proper parameterization schemes, there is a significant uncertainty in the EFs used in air quality and climate models.

In this study, we report the results of laboratory combustion experiments for studying the impact of combustion conditions on the emissions of CO, CO₂, NO, and PM air pollutants. African biomass samples representative of solid fuels used in sub-Saharan African households were combusted under various burning conditions. We quantified the impacts of burning the same fuel under a variety of burning conditions on the resulting emissions, and also examined burning different fuels under the same conditions.

2. Materials and Methods

2.1. Sample Preparation and Burning Setup

Six different sub-Saharan African fuels and a native eastern North American fuel (white pine), with local/scientific names, and fuel sampling locations are listed in Table 1, were used for this study. African fuels were collected from Ethiopia and Botswana, whereas the North American fuel was collected locally in North Carolina. All the fuels were stored in a fume hood for drying and fuel moisture content was estimated before the experiments by measuring mass loss in the fuel due to overnight heating in the oven set at 90°C, as in previous studies (Christian et al., 2003; Pokhrel et al., 2021). The estimated fuel moisture content (expressed as dry basis %) in this study was below 10% for all fuels.

The elemental composition of the fuel was measured by using a carbon, hydrogen, and nitrogen (CHN) analyzer (CHN analyzer 2400 series II, PerkinElmer) that employs the Pregl-Dumas method. Each biomass sample was converted into fine dust using a saw then about 5 mgs of the fine powder was weighed on a tin capsule and crimped with tweezers. These capsule samples were placed inside the autosampler wheel and

Table 1
The As-Received Elemental Composition of Wood Fuel Samples Used in This Work

Sampling location	Local/common name	Scientific name	Elemental composition (%)		
			C	H	N
Botswana	Girar/umbrella thorn, flat-top acacia	<i>Acacia abyssinica</i>	45.8	6.7	0.4
Ethiopia	Bahir Zaf/Eucalyptus	<i>Eucalyptus camaldulensis</i>	46.1	6.6	0.3
Botswana	Mopane/balsam tree	<i>Colophospermum mopane</i>	46.4	6.8	0.3
Botswana	Mukusi/African teak	<i>Baikiaea plurijuga</i>	46.6	6.8	0.5
Ethiopia	Woyira/olive	<i>Olea europaea</i>	49.3	6.9	0.2
Botswana	Wanza	<i>Cordia Africana</i>	45.5	6.5	0.5
North Carolina	White Pine	<i>Pinus strobus</i>	46.8	6.8	0.1

were introduced to a high temperature reactor where they were combusted in a temporarily oxygen enriched atmosphere. CO₂, H₂O, and nitrogen oxides produced during combustion were carried by helium gas and passed through a reduction tube where oxides of nitrogen were reduced to molecular nitrogen. Finally, the gases were homogeneously mixed as they passed through the mixing chamber, and the components of the resulting gas mixture were chromatographically separated before being quantified with a thermal conductivity detector. The percentages of elemental composition of carbon, hydrogen, and nitrogen of the dry fuel with moisture content measured in this study are presented in Table 1. Elemental composition was estimated on an as-received basis (with fuel moisture content ~10%). CHN measurements had a manufacturer-specified accuracy of <0.3% and precision of <0.2%.

Biomass combustion was conducted at North Carolina Agricultural and Technical State University (NCAT) indoor burning facility. Details of the burning facility including the details of the tube furnace and the experimental and chamber cleaning procedures are reported in our previous studies (Pokhrel et al., 2021; Smith et al., 2019; Smith, Cui et al., 2020; Smith, Fiddler et al., 2020) and only a brief description is provided here. The schematic of the NCAT burning facility and measurement set up is shown in Figure S1 in the Supporting Information S1 (note that the UV lights shown in Figure S1 in the Supporting Information S1 were not used in this study). Additional details about the operation of the tube furnace are also provided in the Supporting Information S1. Biomass combustion was performed in a tube furnace and the smoke was transported to the environmental chamber by mixing with zero air supplied to the tube furnace at constant flow rate (10 standard liters per minute). The chamber is operated as a “batch reactor” with a fixed volume of 9 m³. The Teflon walls are somewhat flexible, allowing for small changes in volume during injection and sampling, without a change in pressure. The furnace was disconnected from the chamber about 10 min after ignition and a constant flow of make-up gas (typically 4 L min⁻¹ provided by zero air generator) was supplied to the chamber. Measurements of gaseous species and particle size distribution began typically 15 min before combustion took place. Particles appear to be well mixed inside the chamber within 20 min of the combustion, with the size distribution resolving into a lognormal distribution.

Particle size distribution measurements were taken before combustion was initiated and continued for one hour after initiation. Following this, effective density measurements were taken. Measurements of gas-phase species began before combustion and continued over the course of each experiment. These measurements were performed at 1 Hz and averaged over 1-minute intervals.

The temperature of the furnace can be set from room temperature to 1,000°C, but this study used furnace temperatures in the range from 450°C to 800°C. The furnace was set at a fixed temperature and the average modified combustion efficiency (MCE) was measured to determine the combustion type. The temperatures were not chosen to represent a range of combustion temperatures found in actual use in the field. The furnace temperature was different from the combustion temperature of the fire. The furnace temperature was set to initiate ignition and vary the combustion type. This temperature is dependent on type and size of the furnace or other factors. A mixing fan located inside the chamber was turned on for about 15–20 min after combustion. The temperature and relative humidity (RH) inside the chamber were monitored using a hygrometer (Traceable Products, Model 4085; humidity range 5%–95%). The typical temperature in the

chamber during these experiments ranged from 21°C–24°C and RH was below 5%. Following each set of measurements, the chamber was flushed with zero air at a flow rate of 20 L min⁻¹ until the particle mass reached below 2 µg m⁻³ and nitric oxide and ozone concentrations were below 5 ppbv.

2.2. Instrumentation

We measured the different gas phase species emitted from biomass burning as follows. CO₂ and CO concentrations were measured using a CO₂ analyzer (Model 41C Thermo Scientific) and a CO analyzer (Model 48C Thermo Scientific), respectively. These monitors were calibrated before and after the experiments using certified standard gas cylinders (199.7 ppmv for CO and 5,028 ppmv for CO₂ from Airgas National Welders). NO_x were measured with a Monitor Labs analyzer (Model 8840). The NO_x monitor was calibrated using a certified standard gas cylinder (53.12 ppmv for NO from Airgas National Welders). Due to a failure in the catalytic converter in the NO_x monitor, we were limited to only NO measurements in this study. A UV photometric ozone (O₃) analyzer (Model 49 Thermo Electron) was used to measure the O₃ concentrations. The O₃ analyzer was calibrated using a gas titration method (DeMore & Patafiff, 1976). Briefly, O₃ was produced by passing zero air through the generator having a UV lamp (11SC-1, Spectroline) and titrated with NO in a ~30 mL glass mixing ball. The reduction in the NO concentration was measured by the calibrated NO_x monitor, and O₃ concentration was measured based on the loss in the NO concentration.

We measured the particle size distribution in the range of 14–720 nm using a scanning mobility particle sizer (SMPS, TSI). The SMPS consists of an electrostatic classifier (TSI, Model 3080), long differential mobility analyzer (DMA, TSI, Model 3081), and a general-purpose Water-based condensation particle counter (WCPC, TSI, Model 3787). We also measured the size-selected particle effective density (ρ_{eff}) using an aerosol particle mass analyzer (APM, Kanomax Inc., Model 3602) by connecting DMA and APM in series. Briefly, the DMA was used to select the aerosol size based on its electrical mobility and then the size-selected aerosol passed through the APM, which classified the aerosol based on its mass to charge ratio. The WCPC connected downstream of APM was used to measure the concentration of the particles at each mass. During this study, the APM was operated in stepping mode where the rotational speed of the APM was kept constant, and the voltage underwent stepwise changes to produce a series of selected sizes to determine the particle mass distribution. Details of the operation principle of the APM can be found elsewhere (McMurry et al., 2002; Park et al., 2003, 2004). Particle effective density is calculated using:

$$\rho_{\text{eff}} = \frac{6m_p}{\pi d_m^3} \quad (1)$$

where m_p is the particle mass and d_m is the mobility diameter.

An aerosol chemical speciation monitor (ACSM; Aerodyne Research Inc.) was used to measure submicron non-refractory particulate matter (NR-PM) including organics, nitrate, sulfate, ammonium, and chloride. Aerosol from the chamber was sampled into the ACSM through a critical orifice with a diameter of 100 µm at a constant flow rate of 85 ml min⁻¹. The ACSM was calibrated with ammonium nitrate and ammonium sulfate to estimate the ionization efficiencies and relative ionization efficiencies. The recorded data were processed using the ACSM local toolkit (v. 1.6.0.3) for Igor Pro. Details about the ACSM can be found elsewhere (Ng et al., 2011).

2.3. Modified Combustion Efficiency and EF Calculation

Emissions from fires can be impacted by many factors such as fuel geometry, moisture content, and environmental variables (Stockwell et al., 2014) as well as fire-tending practices and cookstove technology. The relative amount of flaming and smoldering combustion is indicated by calculating modified combustion efficiency (MCE) for the fire.

$$\text{MCE} = \frac{\Delta\text{CO}_2}{\Delta\text{CO}_2 + \Delta\text{CO}} \quad (2)$$

where ΔCO_2 and ΔCO are the background-corrected CO_2 and CO molar concentrations, respectively (Stockwell et al., 2014; Yokelson et al., 1997, 2009). Background concentrations were measured before the ignition of each burn. Though higher MCE values are attributed to more complete combustion, flaming and smoldering can happen simultaneously. Typically, an MCE of ~ 0.8 is attributed to purely smoldering, an MCE of ~ 0.9 represents roughly equal amounts of flaming and smoldering, and an MCE of ~ 0.99 is attributed to purely flaming combustion (Stockwell et al., 2014). The reported MCE values represent a fire average integrated over all stages of combustion, since smoke was introduced into the chamber sampling the entire burn, and measurements from the chamber could not distinguish between different stages.

The EF is defined as the amount of pollutant released per unit mass of the fuel burned. EFs are reported on dry fuel basis. We calculated EFs using the carbon mass balance approach; assuming all of the carbon had been measured and all of the burned carbon was volatilized (Selimovic et al., 2018; Stockwell et al., 2014; Yokelson et al., 1999, 2009):

$$\text{EF}(X) \left(\text{g kg}^{-1} \right) = F_C \times 1000 \times \frac{\text{MW}_X}{\text{MW}_C} \times \frac{\Delta X}{\Delta\text{CO} + \Delta\text{CO}_2} \quad (3)$$

where F_C is the fuel carbon content; MW_C is the molecular weight of carbon; MW_X is the molecular weight of species X ; ΔCO , ΔCO_2 , and ΔX are the background corrected mixing ratios of CO , CO_2 , and species X . Due to limitations in our capability to measure non- CO_2 and non- CO carbon emissions, we neglected the carbon emissions other than CO and CO_2 in the denominator of Equation 3. This may lead to overestimation of EFs by a few percent (Akagi et al., 2011; Andreae & Merlet, 2001). However, this source of error is negligible compared to other sources of error, such as variations in burning conditions, moisture content, fuel type differences, etc. The mass ratio of PM to CO for the each experiment was estimated to determine the EF of PM mass. The mass ratio of background-corrected PM to the background-corrected CO was multiplied by the EF of CO to determine the EFs of PM (g kg^{-1}) (Stockwell et al., 2016). Similarly, total particle number (PN) EFs ($\# \text{kg}^{-1}$) were calculated by multiplying the ratio of PN to the CO mass concentration by the EF of CO . Since number concentrations inside the chamber change rapidly due to diffusional loss, coagulation, and gravitational settling, we corrected those losses based on the first order decay rate of the total number concentration, as shown in Figure S2 in the Supporting Information S1.

2.4. Particulate Mass Measurement

We converted the particle volume distribution measured by the SMPS to PM mass by multiplying the particle volume with the effective density of the particle. In this study, the SMPS sampled from 14–720 nm and in-software multiple charging correction was applied. We found that ρ_{eff} was size independent for burns with $\text{MCE} < 0.9$ (Pokhrel et al., 2021), so for burns with $\text{MCE} < 0.9$, we used the average value of ρ_{eff} calculated from 4–6 different sizes. For burns with $\text{MCE} > 0.9$, ρ_{eff} shows a size dependence, with smaller values of ρ_{eff} for larger mobility sizes. So, for $\text{MCE} > 0.9$ cases, we used the mass mobility exponent relationship to estimate the ρ_{eff} at a desired mobility diameter. The mass mobility exponent relation is expressed as a power-law relationship between m_p and d_m :

$$m_p = C d_m^{D_{\text{fm}}} \quad (4)$$

where C is a pre-factor and D_{fm} is the mass mobility exponent (Park et al., 2003, 2004; Pokhrel et al., 2021). On combining Equations 1 and 4, ρ_{eff} can be expressed as:

$$\rho_{\text{eff}} = \frac{6C d_m^{D_{\text{fm}}}}{\pi d_m^3} = C' d_m^{D_{\text{fm}} - 3} \quad (5)$$

where $C' = \frac{6C}{\pi}$ is a constant. Based on Equation 4, we first estimated the mass mobility exponent and the pre-factor then applied those values in Equation 5 to estimate the ρ_{eff} at a particular size. We set the upper limit of ρ_{eff} as 2 g cm^{-3} (which is assigned as the density of primary particles) as in a previous study (Maricq and Xu, 2004). One representative example of ρ_{eff} calculated for a set of DMA midpoint diameters is shown in Figure S3 in the Supporting Information S1 and the details of the mass estimation is explained in the Supporting Information S1.

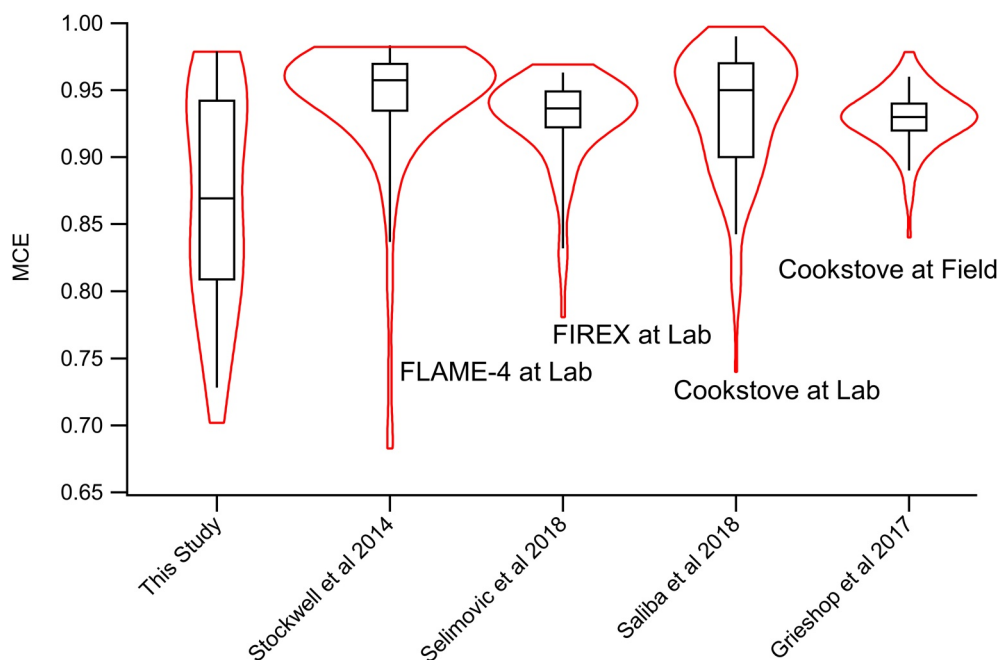


Figure 1. Violin plots showing comparison of modified combustion efficiency (MCE) for previous laboratory and field studies of biomass burning and cookstove emissions. Boxes represent the interquartile range with whiskers as the 95th and fifth percentile of the data and the line inside the box is the median. Violins (area enclosed by red lines) represent the kernel density to show the distribution of MCE.

ACSM measurements were used to estimate the mass of NR-PM. A recent study (Lim et al., 2019) found that the aerosol mass spectrometer collection efficiency depends on the aerosol volatility, with collection efficiencies ranging from 0.35 to 0.64. So, the use of a constant collection efficiency would bias the estimated mass concentrations of NR-PM. In addition, due to a slight difference in size range measured by our SMPS (up to 720 nm) and ACSM (up to 1 μm) and a lack of black carbon mass measurements, we did not estimate the collection efficiency of the ACSM. We estimated the mass percentage of organic aerosol (OA), nitrate, sulfate, ammonium, and chloride in NR-PM and used that fraction to estimate the mass of each component based on SMPS mass measurements by assuming black carbon accounts for 5% of the total PM for smoldering-dominated fires (McClure et al., 2020; Pokhrel et al., 2016). Since the fraction of BC mass in flaming-dominated burns is highly variable, we did not estimate the NR-PM mass for those burns. The mass of NR-PM estimated this way might have some bias if the black carbon mass is more or less than 5% of the PM mass.

3. Results and Discussion

3.1. Simulation of Biomass Burning at Lab

Seven different fuels were burned under various conditions as indicated by the MCE of each burn, as discussed in Section 2.3. Even though the MCE can be influenced by other factors besides furnace temperature, we only adjusted the furnace temperature in this study to create different burning conditions. Figure 1 shows the distribution of the MCE of the different burns in this study and a comparison with previous laboratory and field studies of open BB and cookstove emissions (Grieshop et al., 2017; Saliba et al., 2018; Selimovic et al., 2018; Stockwell et al., 2014). We use MCE as a proxy for burning condition and a basis for comparison because it shows a good correlation with emissions of different gaseous and particulate pollutants and is used extensively in EF measurement studies (Akagi et al., 2011; Bilsback et al., 2019; Champion et al., 2017; Christian et al., 2003; Liu et al., 2017; Selimovic et al., 2018; Stockwell et al., 2014; Yokelson et al., 1997, 2008, 2013). In comparing a few representative laboratory experiments and field studies, the MCE for the laboratory studies is skewed towards flaming conditions (MCE > 0.92 or above), as shown by a very narrow width of the violin plot below MCE = 0.9. Even though a field study of cookstove emissions

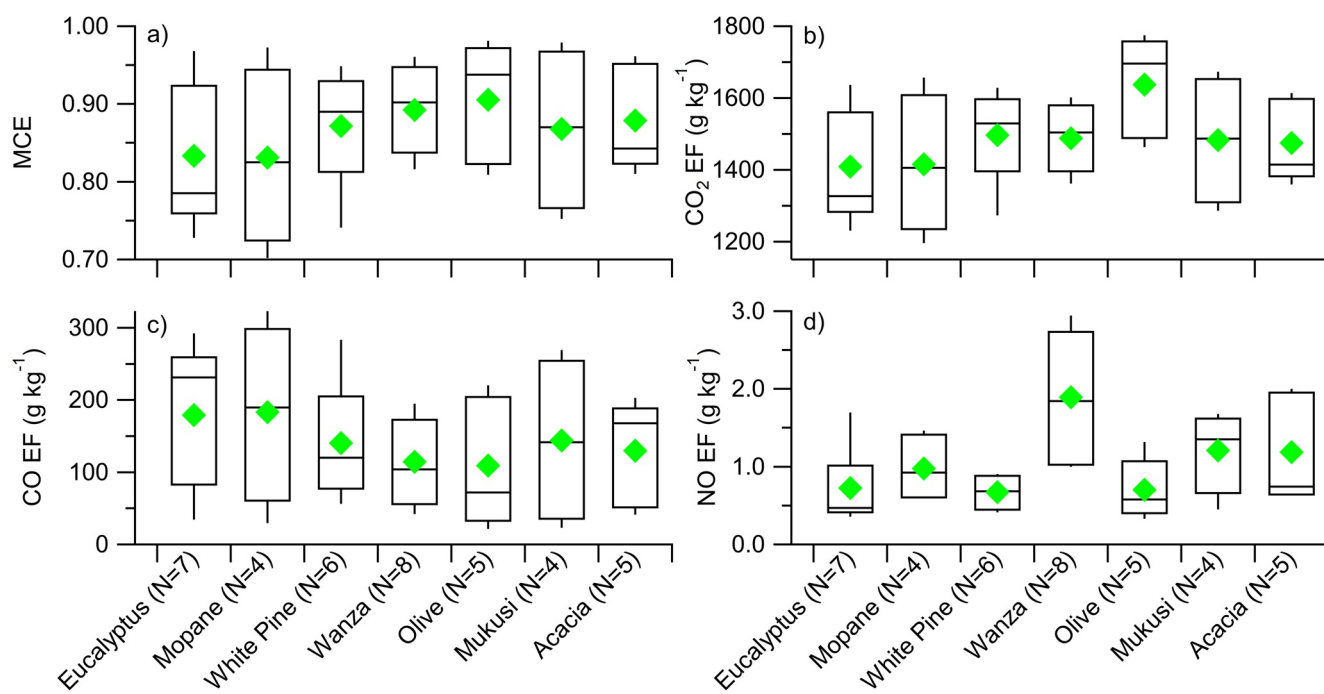


Figure 2. Box and whisker plots of (a) modified combustion efficiency (MCE), (b) emission factor (EF) of CO₂, (c) EF of CO, and (d) EF of NO for the different fuels listed on the bottom axis. Numbers inside the parentheses on the bottom axis represent the number of burns for each fuel type. Boxes represent the interquartile range with whiskers as the 95th and fifth percentile of the data. The line inside the box is the median and the green diamonds are the mean values of the data.

shown in Figure 1 is dominated by high MCE, this is not always the case, as shown by a recent cookstove field study (Eilenberg et al., 2018). In addition, there are field studies observing smoldering wildfires (Barker et al., 2020; Collier et al., 2016) and, as recommended in a recent review article (Hodshire et al., 2019), more laboratory studies of smoldering fires are needed to study the emission behavior under lower MCE conditions. This suggestion is further supported by the recent study based on the airborne field campaign of western US wildfires, which found significant numbers of fires having MCE below 0.9 (as low as 0.85) (Permar et al., 2021).

Conventional ways of burning biomass in a laboratory, such as using cookstoves, typically provide better control over burning conditions than what is found in field measurements, but flaming combustion dominates in these experiments. This skews laboratory studies in examining flaming fires, as shown in Figure 1. More laboratory studies targeting smoldering combustion are needed. With this in mind, we designed experiments to conduct burns of biomass fuels for a wider and uniformly distributed range of MCE values, as shown in Figure 1. As indicated by the width of the violin plot, we were able to conduct burns of biomass fuels from a nearly purely smoldering to a nearly purely flaming condition in a more controlled way. As explained in more details under Section 3.2, despite using seven different fuels, we were able to burn all the fuels within a similar range of MCE values. This fact suggests that conducting combustion studies of biomass fuels in a tube furnace could be a useful and flexible approach to study emissions from BB as a function of burning conditions (Kim et al., 2018).

3.2. Emission of Gas-Phase Species

We conducted a total of 39 different burning experiments with at least 4 burns for each fuel type, as shown in the axis labels of Figure 2. The distribution of the MCE for each fuel type is shown in Figure 2a. The MCE values observed in this study from all fuels were between 0.702 and 0.981 with an average (standard deviation) value of 0.870 (0.080). These values are consistent with previous laboratory experiments for biomass burning (McMeeking et al., 2009; Selimovic et al., 2018; Stockwell et al., 2014) as well as for cookstove emissions (Bilsback et al., 2018; Saliba et al., 2018). For each fuel, the interquartile range of the MCE is

Table 2

Average Modified Combustion Efficiency and Emission Factor (g kg⁻¹) of Different Fuels

Fuel	MCE	CO ₂ EF	CO EF	NO EF
Acacia	0.88 (0.07)	1474 (114)	129 (72)	1.19 (0.70)
Eucalyptus	0.83 (0.09)	1408 (157)	179 (100)	0.72 (0.48)
Mopane	0.83 (0.11)	1415 (168)	183 (107)	0.98 (0.44)
Mukusi	0.87 (0.09)	1483 (156)	143 (99)	1.21 (0.53)
Olive	0.91 (0.07)	1637 (125)	109 (79)	0.703 (0.39)
Wanza	0.89 (0.05)	1487 (89)	114 (57)	1.89 (0.82)
White Pine	0.87 (0.07)	1497 (118)	140 (75)	0.67 (0.23)

Note. Values inside the parentheses represent one standard deviation of the average.

slightly different, but the average MCE for each fuel type lies within one standard deviation of the average for all fuels, as shown in Table 2. The data for individual burning experiments are provided in Table S1 in the Supporting Information S2.

Like the MCE, we also observed a similar range of EFs of CO₂ and CO for all fuels, as shown in Figures 2b and 2c. Not surprisingly, EFs show a good correlation for CO₂ and anticorrelation for CO with the MCE values, as observed in a previous study (Selimovic et al., 2018). The estimated ranges of CO₂ EFs based on all burning experiments lies between 1,196 g kg⁻¹ to 1,775 g kg⁻¹ with an average (standard deviation) value of 1,484 (146) g kg⁻¹ and that of CO lies between 21.39 g kg⁻¹ to 323.09 g kg⁻¹ with an average (standard deviation) value of 141.38 (86.98) g kg⁻¹. These values lie within the range of EFs of CO₂ and CO for open cooking found in a previous study (Akagi et al., 2011). The average of CO₂ and CO EFs based on each fuel type are shown in Table 2.

Unlike CO₂, the EF of CO is highly sensitive to the burning conditions, with an order of magnitude increase when the MCE value changes from ~0.95 to ~0.75 for the same fuel. Variations in CO EFs found in different cookstove types (Grieshop et al., 2017; Roden et al., 2006; Wathore et al., 2017) are due to differences in fuel burning efficiencies, which can be influenced by factors other than cookstove type (Stockwell et al., 2014). These could include fuel dryness, surface area, fire-tending, stove operation, and fuel type. We compare our estimated values of CO₂ and CO EFs with previous laboratory studies (Selimovic et al., 2018; Stockwell et al., 2014) for a wide variety of fuels as well as a field study focusing on African BB emissions (Barker et al., 2020). In addition, we also compare the CO EFs with previous cookstove emission studies (Eilenberg et al., 2018; Grieshop et al., 2017). As shown in Figure S4a and S4b in the Supporting Information S1, our estimated values compare well with previous studies and show a similar correlation between MCE and EFs of CO₂ and CO.

The range of NO EFs found in this study lie between 0.33 g kg⁻¹ and 2.95 g kg⁻¹ with an average (one standard deviation) value of 1.11 (0.71) g kg⁻¹, which compares well with the NO EF for open cooking (1.42 (0.42) g kg⁻¹) found in a previous study (Akagi et al., 2011). Like CO₂ and CO, we also compared the NO EFs with previous laboratory studies (Selimovic et al., 2018; Stockwell et al., 2014) and found NO EFs derived from African fuels are consistent with those from western US, as shown in Figure S4c in the Supporting Information S1. Like in previous studies, we did not observe a good correlation of NO EFs with the MCE. Unlike CO₂ and CO, NO EFs show a fuel type dependence, with some fuels showing consistently higher values than others. For a similar range of MCE, NO EFs for wanza are consistently higher than most of the other fuels, as shown in Table 2. As evident from Figure 2d, NO EFs for eucalyptus, white pine, and olive are relatively lower than the rest of the fuels, which aligns well with the relatively lower fuel nitrogen content of those fuels, as shown in Table 1. This result is consistent with previous studies concluding that NO emission is partly dependent on the fuel nitrogen content (Andreae & Merlet, 2001; McMeeking et al., 2009; Tihay-Felicelli et al., 2017).

We performed a multiple regression of NO EFs as a function of MCE and fuel nitrogen content. Multiple regression analysis significantly improves the correlation with an r^2 increase from 0.41 obtained from simple linear regression with respect to MCE to 0.70 with MCE and nitrogen content. This fact suggests that the incorporation of fuel nitrogen content can significantly improve the prediction of NO EFs and that MCE and nitrogen content accounts for 70% of the NO EF dependence. Details of the regression analysis are presented in the supplementary information. Furthermore, we also explored the impact of combustion condition on NO emission by burning the same fuel under various combustion conditions indicated by the MCE values. For the same fuel (wanza), the NO EF shows a good correlation with MCE value, with larger NO emissions for flaming condition and lower emissions for smoldering conditions. On changing the MCE from ~0.81 to ~0.96, the NO EF increased by the factor of 3, as shown in Figure S5 in the Supporting Information S1. EFs of gas phase species for all burns are provided in Table S1 in the Supporting Information S2.

3.3. Emission of Particulate Matter

Like EFs of CO, EFs of PM mass also show large variations, with estimated values ranging from 0.82 g kg^{-1} to 25.10 g kg^{-1} for different burning conditions. Given such a large variation in EFs (almost two orders in magnitude) and no obvious discrepancies between different fuel types, we parameterized EFs of PM mass with MCE. EFs of PM mass shows good correlation ($r^2 = 0.76$) with MCE (as shown in Figure S6 in the Supporting Information S1) having larger PM emissions for smoldering fires and lower PM emissions for flaming fires. Typically, for flaming-dominated fires ($\text{MCE} > 0.95$) the estimated EFs of PM are less than 5 g kg^{-1} , indicating that efficient burning can significantly reduce PM emissions. We compare our results with previous laboratory and field studies (Eilenberg et al., 2018; Grieshop et al., 2017; Hosseini et al., 2013; Jayaraman et al., 2018) of cookstove and biomass burning emissions and found a consistent relationship. There is some scatter in the data where some data points fall outside the 95% confidence interval of the best fit line, particularly for $\text{MCE} > 0.9$, but in general, the relationship is consistent. The PM mass calculated in this study is $\sim \text{PM}_{0.72}$ because the upper limit of the SMPS used in this work was 720 nm, but an insignificant fraction of particles measured were $> 600 \text{ nm}$. Most of the data from previous studies presented in Figure S6 in the Supporting Information S1 are for $\text{PM}_{2.5}$, but for fresh BB emissions, these ranges of PM may be used interchangeably (Akagi et al., 2011), because the majority of the PM mass (80%–90%) comes from diameters less than $1 \mu\text{m}$ (Reid et al., 2005). From an air pollution perspective, PM is considered a main pollutant indicator. There have been numerous cookstove emission studies focused on emissions of PM and other gaseous pollutants, and the variabilities in the estimated PM EFs values are often attributed to the impacts of stove types, fuel moisture conditions or fuel types (Bilsback et al., 2018, 2019; Champion et al., 2017; Coffey et al., 2017; Corbin et al., 2015; de la Sota et al., 2017; Du et al., 2017; Eilenberg et al., 2018; Grieshop et al., 2017; Islam et al., 2021; Mitchell et al., 2019; Mutlu et al., 2016; Pandey et al., 2017; Roden et al., 2006; Wathore et al., 2017). Due to large variations in reported EFs of PM without adequate parameterization, there remains a challenge in representing those emissions in models.

A recent review article on stove intervention programs in low- and middle-income countries found that there were more available measurements of CO than PM (Thomas et al., 2015). This could potentially be due to the fact that CO is substantially easier to measure with portable instruments compared to PM. There are a few studies which proposed a correlation between CO and PM EFs (Champion et al., 2017; Grieshop et al., 2017; Roden et al., 2009), but that relationship depends on many factors including the type of stove, fuel combusted, and fuel moisture content (Carter et al., 2017). With that in mind, we parameterized EFs of PM as a function of EFs of CO based on this study. As shown in Figure 3, EFs of PM show a good positive correlation ($r^2 = 0.78$) with EFs of CO from the data measured in this study. In addition, the slope of the regression ($0.102 (0.023) \text{ g g}^{-1}$), which also represents the emission ratio of PM with CO, compares well with the 11-year average PM emission ratio with CO ($0.109 (0.01) \text{ g g}^{-1}$) measured at Boise, ID (McClure and Jaffe, 2018) during a western US wildfire season. The intercept of the regression line is statistically insignificant (p value = 0.12), supporting the fact that for complete combustion (at CO = 0) there is no production of particulate matter. We compared the regression based on this study with the data from previous studies. Data from the literature includes 11 different studies (Coffey et al., 2017; Du et al., 2017; Eilenberg et al., 2018; Grieshop et al., 2017; Islam et al., 2021; Jetter et al., 2012; MacCarty et al., 2010; Mutlu et al., 2016; Roden et al., 2006, 2009; Wathore et al., 2017) with different fuels (dry and wet wood, dung, coconut shells, and biomass briquette); varieties of stoves types and 405 different field measurements from the south and east Asia, different parts of Africa, and laboratory studies (Table S2 in the Supporting Information S2). As evident from Figure 3, regardless of all the aforementioned variabilities, the majority (65%) of the literature data fall within the 95% confidence interval of the regression line. In this work, a correlation was found for CO and PM emissions generated by combustion of seven wood fuels with moisture content (dry basis) $< 10\%$ in a tube furnace and measured in a laboratory chamber with temperatures $\sim 21\text{--}24^\circ\text{C}$ and RH below 5%. We also examined the predictive capabilities of our regression model. Based on the EFs of CO, we estimated the EFs of PM and found that predicted EFs of PM compared well with the measured literature values. The majority of the predicted EFs of PM lie close to the measured values as evident by highly dense data points around the one-to-one line, as shown in scatter density plot between predicted and measured EFs of PM (Figure S7 in the Supporting Information S1). The mean bias error, mean absolute error, and root mean square error of the EF of PM are found to be 0.62 g kg^{-1} , 2.35 g kg^{-1} , and 3.24 g kg^{-1} respectively. This relation is not always consistent, and should be limited to controlled laboratory and cookstove

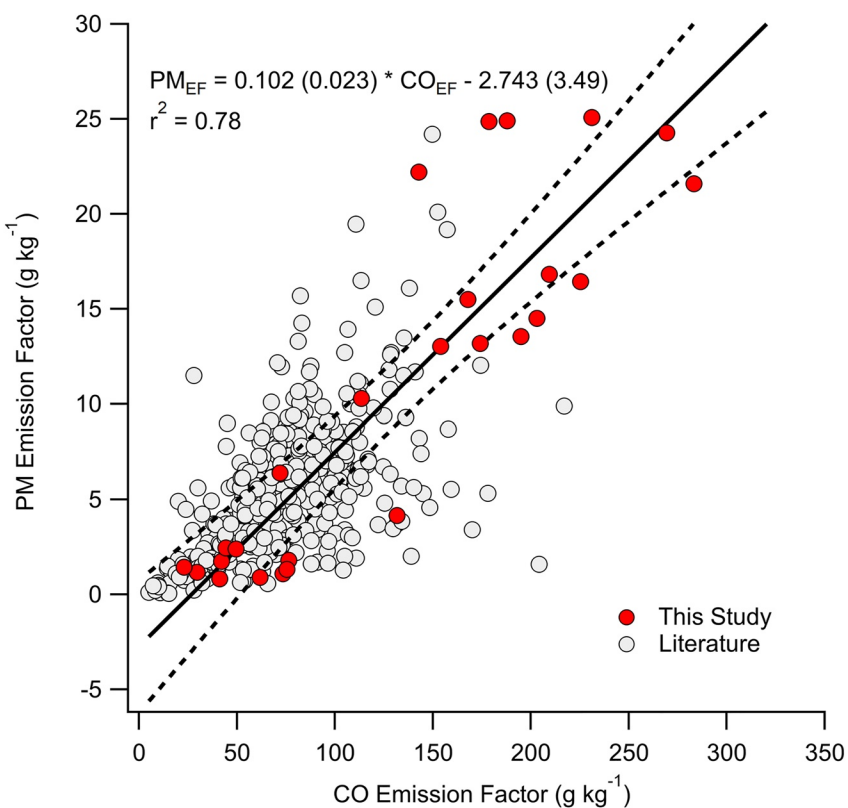


Figure 3. The particulate matter emission factor (EF) plotted as a function of CO EF. The solid black line (equation and r^2 value) is the linear best fit based on this study and the dotted black lines are the 95% confidence interval of the fit based on this study. Also included (gray filled circle) are data from previous studies. Original data and references for all the studies are provided in the Supporting Information S1. The regression equation for the literature data is $PM_{EF} = 0.060 (0.004) \times CO_{EF} + 1.092 (0.0348)$ with an r^2 value of 0.334.

emission studies using wood samples. A recent comprehensive review article (Carter et al., 2017) examined the PM-CO relationship in household energy studies for mostly wood fuels, though some other fuels were included. Their results suggest that although PM-CO correlations were found in some studies, “results suggest that exposure to CO is not a consistently valid surrogate measure of exposure to PM_{2.5}.” Fuel and stove type dependent studies to validate the use of CO EF as a proxy to PM EF should be conducted to validate these results (Carter et al., 2017). It is likely that, though our parametrization encompasses the majority of individual measurements, trends are not consistently found within each of the aforementioned studies.

Besides PM measured by the SMPS, we also reported the EFs of NR-PM measured by the ACSM. EFs of NR-PM as a function of MCE are shown in Figure 4, which also compares the NR-PM EFs from a previous study (May et al., 2014). As stated earlier in Section 2.4, we only presented that data for smoldering fires (MCE ~ 0.9 and lower). OA is the major particulate species emitted ($>90\%$ by mass in most of the burns) and has an order of magnitude higher EFs compared with the inorganic species. Such a high OA fraction has also been observed for smoldering fires in previous studies (Liu et al., 2017). The estimated average OA EF ($15.33 \pm 7.23 \text{ g kg}^{-1}$) is in good agreement with the previous study (May et al., 2014), which was measured during the prescribed montane fires ($11.2 \pm 2.7 \text{ g kg}^{-1}$). However, OA EFs in this study are significantly larger than chaparral and costal fire EF values measured by May et al. (2014); potentially due to the larger observed MCE during those fires. Similar to total PM, EFs of OA show a burning-condition dependence with higher EF for the emissions with lower MCE. Besides OA, the inorganic nonrefractory species measured by the ACSM includes sulfate, nitrate, ammonium, and chloride. The estimated average EFs of inorganic nonrefractory species are $0.032 (0.026)$, $0.16 (0.08)$, $0.034 (0.067)$, and $0.090 (0.175) \text{ g kg}^{-1}$ for sulfate, nitrate, ammonium, and chloride respectively. Although these values are comparable with the previous study of fuels from the south east coastal plain (May et al., 2014), western US wildfires typically have

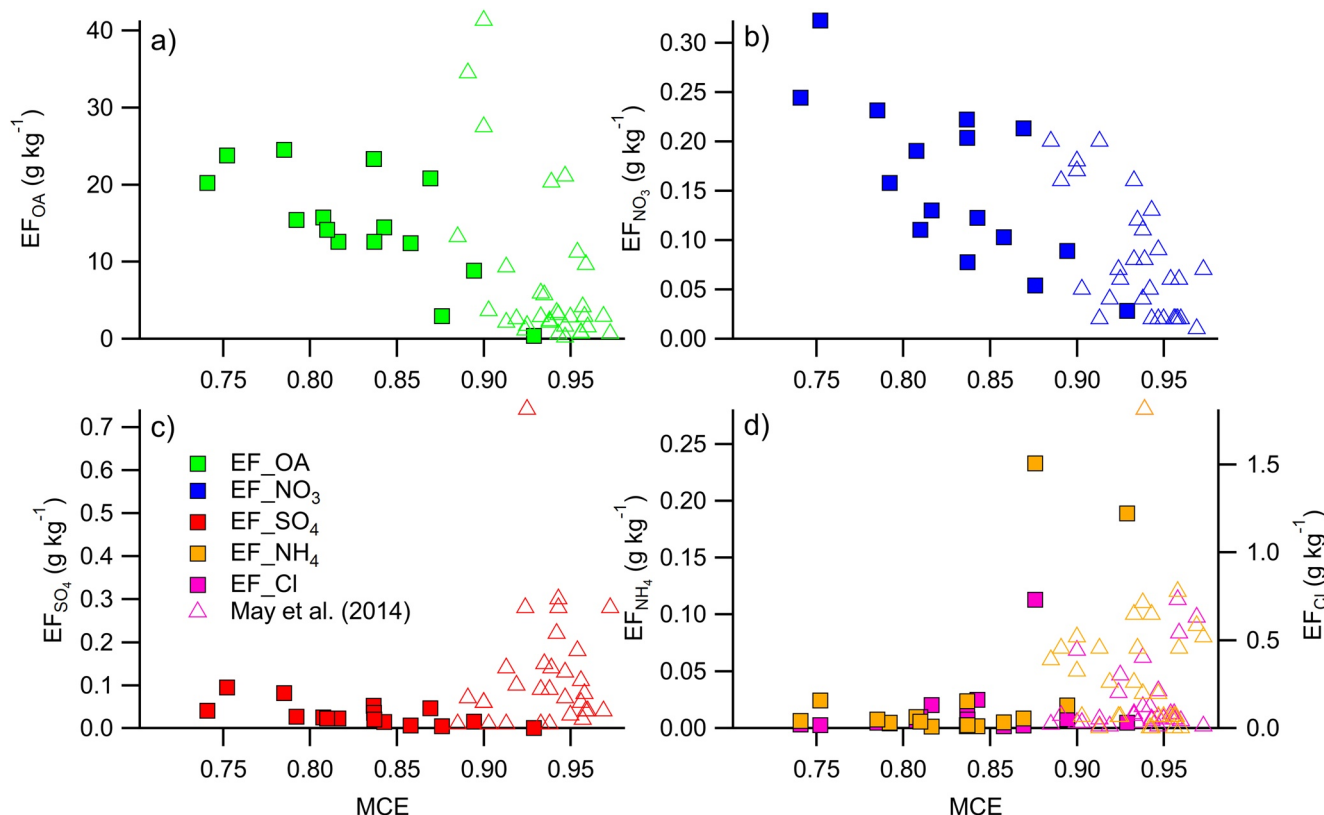


Figure 4. Emission factors of submicron aerosol species plotted as function of modified combustion efficiency (MCE) for (a) organic aerosol, (b) nitrate, (c) sulfate, and (d) ammonium and chloride. Also included (open triangles) are the data from May et al. (2014) that is based on laboratory and airborne measurements. The data for the Figure is provided in Table S1 in the Supporting Information S2.

larger values (Liu et al., 2017). This could potentially be due to fuel type dependence, as suggested in previous studies (Christian et al., 2003; Hosseini et al., 2013; May et al., 2014). Unlike OA, EFs of nonrefractory inorganic species do not show dependence on burning conditions (as quantified by the MCE) except nitrate, which has also been observed in previous studies (May et al., 2014; McMeeking et al., 2009).

Besides particle mass, we also estimated the EF of particle number emitted during combustion. Like PM mass EFs, PN EFs also show dependence on burning conditions, with smoldering fire emitting an order of magnitude larger PN compared to flaming fires, as shown in Figure 5. The range of PN EFs found in this study lies between $0.38 \times 10^{15} \text{ kg}^{-1}$ to $14.8 \times 10^{15} \text{ kg}^{-1}$ with an average value of $7.18 (4.16) \times 10^{15} \text{ kg}^{-1}$. Unlike mass, the number EF shows a weak correlation with MCE as quantified by the r^2 value of 0.54. All the EFs and MCE values for each burn are provided in Table S1 in the Supporting Information S2. Janhäll et al. (2010) reported PN EFs for different wildfires and a decrease in PN EF with increasing MCE was observed in this work and our work, though our values were consistently higher. This could potentially be due to the fact that aircraft measurements of ambient smoke might not sample fresh ($t \sim 0$ minute) smoke and we may have sampled smaller particle sizes. Instruments used in their study were limited to particles greater than 100 nm in size. Our values are consistent with a previous laboratory study of different BB samples, with an estimated range of PN EFs between $2.88 (2.82) \times 10^{15} \text{ kg}^{-1}$ to $24.41 (22.85) \times 10^{15} \text{ kg}^{-1}$ (Bhattacharai et al., 2018). The values inside the parentheses represent one standard deviation about the average.

4. Conclusions

We studied the emissions from seven different fuels (six African fuels and one eastern US native fuel) under a wide variety of burning conditions that range from purely smoldering to flaming, as indicated by the resulting MCE values. We quantified the EFs of gases (carbon dioxide, carbon monoxide, and nitric oxide),

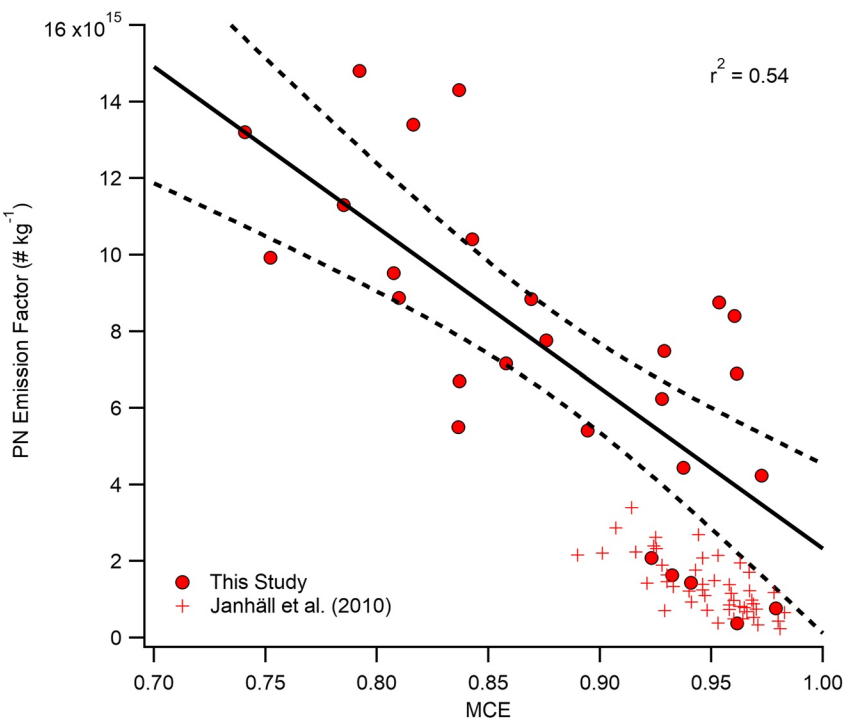


Figure 5. The particle number emission factor (EF) plotted as a function of modified combustion efficiency. Also included are the particle number EFs from a previous study, as shown in legend. The solid black line is the best linear fit of the data from this study and the dotted black lines are 95% confidence intervals of the fit from this study.

particulate mass and number as well as nonrefractory particulate matter constituents. The range of MCE observed in this study for all fuels lies between 0.702 to 0.981, with an average (standard deviation) value of 0.870 (0.080). Regardless of fuel types and origin, the range of MCE values was similar for all fuels, resulting from similar ranges for values for CO and CO₂ EFs. The estimated range of CO₂ EFs based on all burning experiments lies between 1,196 g kg⁻¹ and 1,775 g kg⁻¹ with an average (one standard deviation) value of 1,484 (146) g kg⁻¹. The CO EF range lies between 21.39 g kg⁻¹ and 323.09 g kg⁻¹ with an average (one standard deviation) value of 141.38 (86.98) g kg⁻¹.

The range of NO EFs found in this study lies between 0.33 g kg⁻¹ and 2.95 g kg⁻¹ with an average (one standard deviation) value of 1.11 (0.71) g kg⁻¹, which shows a fuel type dependency with consistency higher EFs for fuels with higher nitrogen content. Even though NO EFs show a poor correlation with MCE, the incorporation of fuel nitrogen content in a multiple regression scheme significantly improves the correlation. The fit r^2 value goes from 0.41 to 0.70 upon inclusion of nitrogen content information, suggesting its incorporation can significantly improve the prediction of NO EFs. For the same fuel, emissions of NO show strong positive dependence on MCE ($r^2 = 0.91$) and NO EFs increase by a factor of 3 with a change in MCE from ~ 0.81 to ~ 0.96 .

Although EFs of PM mass and OA show good correlation with MCE, nonrefractory inorganic species do not show a dependence on MCE. We found that the EF of PM mass is inversely correlated with MCE and changes by a factor of 30 between purely flaming and purely smoldering conditions (ranging from 0.82 g kg⁻¹ to 25.10 g kg⁻¹, respectively). The results of our regression between PM EFs and CO EFs are reasonably consistent with 11 different cookstove emission studies (Coffey et al., 2017; Du et al., 2017; Eilenberg et al., 2018; Grieshop et al., 2017; Islam et al., 2021; Jetter et al., 2012; MacCarty et al., 2010; Mutlu et al., 2016; Roden et al., 2006, 2009; Wathore et al., 2017) though the strength of this dependence in the literature is highly variable. Like PM mass, the PN EF also shows an MCE dependency, with smoldering fires emitting an order of magnitude higher PN EFs than flaming fires.

As pointed out by a recent review article (Hodshire et al., 2019), all the laboratory studies to date are skewed towards flaming fires which necessitates the study of more smoldering fires. Our combustion setup using

a tube furnace allows us to have more control of burning conditions, with all the fuels burnt with a very similar range of MCE. As shown in Figure 1, the distribution of MCE in our study, ranging from 0.70 to 0.98, is more uniform and encompasses a greater variety of burning conditions than previous laboratory studies. This fact suggests that the burning of fuel in a tube furnace would be a useful and flexible experimental approach to study BB emission under controlled burning conditions.

Data Availability Statement

Laboratory data used to generate the figures is available at Pokrrel, Rudra; Fiddler, Marc N.; Gordon, Janica; Bililign, Solomon (2021): SI_Tables (2).xlsx. figshare. Data set. <https://doi.org/10.6084/m9.figshare.14669412.v1>.

Acknowledgments

We are thankful to Analytical Services Laboratory of College of Agriculture and Environmental Sciences at North Carolina Agriculture and Technical State University for the elemental analysis of wood samples. The authors are immensely grateful to Dr. Kiran Subedi for providing his expertise that greatly assisted the organic compositional analysis of our samples. The ACSM system was kindly provided by RTI International. The calibration and subsequent system verification of the ACSM was done by Drs. Prakash Doraiswamy (RTI) and Karsten Baumann (UNC Chapel Hill), whose contribution we gratefully appreciate and acknowledge. This work is supported by NSF grant # AGS1831013. J. Gordon acknowledges the partial support by the Department of Education under the Title III HBGI grant. Any opinions, findings, and conclusions, or recommendations expressed in this material are those of the author(s) and do not necessarily reflect the views of the Department of Education.

References

Adkins, E., Tyler, E., Wang, J., Siriri, D., & Modi, V. (2010). Field testing and survey evaluation of household biomass cookstoves in rural sub-Saharan Africa. *Energy for Sustainable Development*, 14(3), 172–185. <https://doi.org/10.1016/j.esd.2010.07.003>

Akagi, S. K., Yokelson, R. J., Wiedinmyer, C., Alvarado, M. J., Reid, J. S., Karl, T., et al. (2011). Emission factors for open and domestic biomass burning for use in atmospheric models. *Atmospheric Chemistry and Physics*, 11(9), 4039–4072. <https://doi.org/10.5194/acp-11-4039-2011>

Andreae, M. O. (2019). Emission of trace gases and aerosols from biomass burning—An updated assessment. *Atmospheric Chemistry and Physics*, 19(13), 8523–8546. <https://doi.org/10.5194/acp-19-8523-2019>

Andreae, M. O., & Merlet, P. (2001). Emission of trace gases and aerosols from biomass burning. *Global Biogeochemical Cycles*, 15(4), 955–966. <https://doi.org/10.1029/2000gb001382>

Assamoi, E.-M., & Liousse, C. (2010). A new inventory for two-wheel vehicle emissions in West Africa for 2002. *Atmospheric Environment*, 44(32), 3985–3996. <https://doi.org/10.1016/j.atmosenv.2010.06.048>

Barker, P. A., Allen, G., Gallagher, M., Pitt, J. R., Fisher, R. E., Bannan, T., et al. (2020). Airborne measurements of fire emission factors for African biomass burning sampled during the MOYA campaign. *Atmospheric Chemistry and Physics*, 20(23), 15443–15459. <https://doi.org/10.5194/acp-20-15443-2020>

Beltramo, T., & Levine, D. I. (2013). The effect of solar ovens on fuel use, emissions and health: Results from a randomised controlled trial. *Journal of Development Effectiveness*, 5(2), 178–207. <https://doi.org/10.1080/19439342.2013.775177>

Beyene, A. D., & Koch, S. F. (2013). Clean fuel-saving technology adoption in urban Ethiopia. *Energy Economics*, 36, 605–613. <https://doi.org/10.1016/j.eneco.2012.11.003>

Bhattarai, C., Samburova, V., Sengupta, D., Iaukea-Lum, M., Watts, A. C., Moosmüller, H., & Khlystov, A. Y. (2018). Physical and chemical characterization of aerosol in fresh and aged emissions from open combustion of biomass fuels. *Aerosol Science and Technology*, 52(11), 1266–1282. <https://doi.org/10.1080/02786826.2018.1498585>

Bilsback, K. R., Dahlke, J., Fedak, K. M., Good, N., Hecobian, A., Herckes, P., et al. (2019). A laboratory assessment of 120 air pollutant emissions from biomass and fossil fuel cookstoves. *Environmental Science & Technology*, 53(12), 7114–7125. <https://doi.org/10.1021/acsest.8b07019>

Bilsback, K. R., Eilenberg, S. R., Good, N., Heck, L., Johnson, M., Kodros, J. K., et al. (2018). The Firepower Sweep Test: A novel approach to cookstove laboratory testing. *Indoor Air*, 28(6), 936–949. <https://doi.org/10.1111/ina.12497>

Bond, T. C., Bhardwaj, E., Dong, R., Jogani, R., Jung, S., Roden, C., et al. (2007). Historical emissions of black and organic carbon aerosol from energy-related combustion. *Global Biogeochemical Cycles*, 21(2), GB2018. <https://doi.org/10.1029/2006GB002840>

Bond, T. C., Doherty, S. J., Fahey, D. W., Forster, P. M., Berntsen, T., DeAngelo, B. J., et al. (2013). Bounding the role of black carbon in the climate system: A scientific assessment. *Journal of Geophysical Research: Atmospheres*, 118(11), 5380–5552. <https://doi.org/10.1002/jgrd.50171>

Bond, T. C., Streets, D. G., Yarber, K. F., Nelson, S. M., Woo, J.-H., & Klimont, Z. (2004). A technology-based global inventory of black and organic carbon emissions from combustion. *Journal of Geophysical Research*, 109, D14203. <https://doi.org/10.1029/2003jd003697>

Carter, E., Norris, C., Dionisio, K. L., Balakrishnan, K., Checkley, W., Clark, M. L., et al. (2017). Assessing exposure to household air pollution: A systematic review and pooled analysis of carbon monoxide as a surrogate measure of particulate matter. *Environmental Health Perspectives*, 125(7), 076002. <https://doi.org/10.1289/EHP767>

Champion, W. M., Connors, L., & Montoya, L. D. (2017). Emission factors of fine particulate matter, organic and elemental carbon, carbon monoxide, and carbon dioxide for four solid fuels commonly used in residential heating by the U.S. Navajo Nation. *Journal of the Air & Waste Management Association*, 67(9), 1020–1035. <https://doi.org/10.1080/10962247.2017.1334717>

Christian, T. J., Kleiss, B., Yokelson, R. J., Holzinger, R., Crutzen, P. J., Hao, W. M., et al. (2003). Comprehensive laboratory measurements of biomass-burning emissions: 1. Emissions from Indonesian, African, and other fuels. *Journal of Geophysical Research*, 108(D23), 4719. <https://doi.org/10.1029/2003jd003704>

Coffey, E. R., Muvandimwe, D., Hagar, Y., Wiedinmyer, C., Kanyomse, E., Piedrahita, R., et al. (2017). New emission factors and efficiencies from in-field measurements of traditional and improved cookstoves and their potential implications. *Environmental Science & Technology*, 51(21), 12508–12517. <https://doi.org/10.1021/acs.est.7b02436>

Collier, S., Zhou, S., Onasch, T. B., Jaffe, D. A., Kleinman, L., Sedlacek, A. J., et al. (2016). Regional influence of aerosol emissions from wildfires driven by combustion efficiency: Insights from the BBOP campaign. *Environmental Science & Technology*, 50(16), 8613–8622. <https://doi.org/10.1021/acs.est.6b01617>

Corbin, J. C., Keller, A., Lohmann, U., Burtscher, H., Sierau, B., & Mensah, A. A. (2015). Organic emissions from a wood stove and a pellet stove before and after simulated atmospheric aging. *Aerosol Science and Technology*, 49(11), 1037–1050. <https://doi.org/10.1080/0278826.2015.1079586>

de la Sota, C., Kane, M., Mazorra, J., Lumbreiras, J., Youm, I., & Viana, M. (2017). Intercomparison of methods to estimate black carbon emissions from cookstoves. *The Science of the Total Environment*, 595, 886–893. <https://doi.org/10.1016/j.scitotenv.2017.03.247>

Delfino, R. J., Brummel, S., Wu, J., Stern, H., Ostro, B., Lipsett, M., et al. (2009). The relationship of respiratory and cardiovascular hospital admissions to the southern California wildfires of 2003. *Occupational and Environmental Medicine*, 66(3), 189–197. <https://doi.org/10.1136/oem.2008.041376>

DeMore, W. B., & Patafopf, M. (1976). Comparison of ozone determinations by ultraviolet photometry and gas-phase titration. *Environmental Science & Technology*, 10, 897–899. <https://doi.org/10.1021/es60120a012>

Du, W., Shen, G., Chen, Y., Zhu, X., Zhuo, S., Zhong, Q., et al. (2017). Comparison of air pollutant emissions and household air quality in rural homes using improved wood and coal stoves. *Atmospheric Environment*, 166, 215–223. <https://doi.org/10.1016/j.atmosenv.2017.07.029>

Eck, T. F., Holben, B. N., Ward, D. E., Mukelabai, M. M., Dubovik, O., Smirnov, A., et al. (2003). Variability of biomass burning aerosol optical characteristics in southern Africa during the SAFARI 2000 dry season campaign and a comparison of single scattering albedo estimates from radiometric measurements. *Journal of Geophysical Research*, 108(D13), 8477. <https://doi.org/10.1029/2002jd002321>

Eilenberg, S. R., Bilsback, K. R., Johnson, M., Kodros, J. K., Lipsky, E. M., Naluwagga, A., et al. (2018). Field measurements of solid-fuel cookstove emissions from uncontrolled cooking in China, Honduras, Uganda, and India. *Atmospheric Environment*, 190, 116–125. <https://doi.org/10.1016/j.atmosenv.2018.06.041>

Elliott, C. T., Henderson, S. B., & Wan, V. (2013). Time series analysis of fine particulate matter and asthma reliever dispensations in populations affected by forest fires. *Environmental Health*, 12(1), 11. <https://doi.org/10.1186/1476-069X-12-11>

Flamant, C., Knippertz, P., Fink, A. H., Akpo, A., Brooks, B., Chiu, C. J., et al. (2018). The dynamics–aerosol–chemistry–cloud interactions in West Africa field campaign: Overview and research highlights. *Bulletin of the American Meteorological Society*, 99(1), 83–104. <https://doi.org/10.1175/bams-d-16-0256.1>

Forouzanfar, M. H., Afshin, A., Alexander, L. T., Anderson, H. R., Bhutta, Z. A., Biryukov, S., et al. (2016). Global, regional, and national comparative risk assessment of 79 behavioural, environmental and occupational, and metabolic risks or clusters of risks, 1990–2015: A systematic analysis for the Global Burden of Disease Study 2015. *The Lancet*, 388(10053), 1659–1724.

Grieshop, A. P., Jain, G., Sethuraman, K., & Marshall, J. D. (2017). Emission factors of health- and climate-relevant pollutants measured in home during a carbon-finance-approved cookstove intervention in rural India. *Geohealth*, 1(5), 222–236. <https://doi.org/10.1002/2017GH000066>

Haywood, J. M., Abel, S. J., Barrett, P. A., Bellouin, N., Blyth, A., Bower, K. N., et al. (2020). Overview: The CLoud-Aerosol-Radiation Interaction and Forcing: Year 2017 (CLARIFY-2017) measurement campaign. *Atmospheric Chemistry and Physics*, 21(2), 1049–1084. <https://doi.org/10.5194/acp-2020-729>

Henderson, S. B., Brauer, M., MacNab, Y. C., & Kennedy, S. M. (2011). Three measures of forest fire smoke exposure and their associations with respiratory and cardiovascular health outcomes in a population-based cohort. *Environmental Health Perspectives*, 119(9), 1266–1271. <https://doi.org/10.1289/ehp.1002288>

Hodshire, A. L., Akherati, A., Alvarado, M. J., Brown-Steiner, B., Jathar, S. H., Jimenez, J. L., et al. (2019). Aging effects on biomass burning aerosol mass and composition: A critical review of field and laboratory studies. *Environmental Science & Technology*, 53(17), 10007–10022. <https://doi.org/10.1021/es502588>

Holstius, D. M., Reid, C. E., Jesdale, B. M., Holstius, D. M., & Morello-Frosch, R. (2012). Birth weight following pregnancy during the 2003 Southern California wildfires. *Environmental Health Perspectives*, 120(9), 1340–1345. <https://doi.org/10.1289/ehp.1104515>

Hosseini, S., Urbanski, S. P., Dixit, P., Qi, L., Burling, I. R., Yokelson, R. J., et al. (2013). Laboratory characterization of PM emissions from combustion of wildland biomass fuels. *Journal of Geophysical Research: Atmospheres*, 118(17), 9914–9929. <https://doi.org/10.1002/jgrd.50481>

Ichoku, C., Ellison, L. T., Willmot, K. E., Matsui, T., Dezfuli, A. K., Gatebe, C. K., et al. (2016). Biomass burning, land-cover change, and the hydrological cycle in Northern sub-Saharan Africa. *Environmental Research Letters*, 11(9), 095005. <https://doi.org/10.1088/1748-9326/11/9/095005>

Ichoku, C., Giglio, L., Wooster, M. J., & Remer, L. A. (2008). Global characterization of biomass-burning patterns using satellite measurements of fire radiative energy. *Remote Sensing of Environment*, 112(6), 2950–2962. <https://doi.org/10.1016/j.rse.2008.02.009>

IEA. (2020). IEA, IRENA, UNSD, World Bank, WHO. 2020. Tracking SDG 7: The Energy Progress Report. World Bank, Washington DC. © World Bank. License: Creative Commons Attribution—NonCommercial 3.0 IGO (CC BY-NC 3.0 IGO).

Islam, M. M., Wathore, R., Zerriffi, H., Marshall, J. D., Bailis, R., & Grieshop, A. P. (2021). In-use emissions from biomass and LPG stoves measured during a large, multi-year cookstove intervention study in rural India. *The Science of the Total Environment*, 758, 143698. <https://doi.org/10.1016/j.scitotenv.2020.143698>

Jacobson, M. Z. (2001). Global direct radiative forcing due to multicomponent anthropogenic and natural aerosols. *Journal of Geophysical Research*, 106(D2), 1551–1568. <https://doi.org/10.1029/2000JD900514>

Janhäll, S., Andreae, M. O., & Pöschl, U. (2010). Biomass burning aerosol emissions from vegetation fires: Particle number and mass emission factors and size distributions. *Atmospheric Chemistry and Physics*, 10(3), 1427–1439. <https://doi.org/10.5194/acp-10-1427-2010>

Jary, H. R., Kachidiku, J., Banda, H., Kapanga, M., Doyle, J. V., Banda, E., et al. (2014). Feasibility of conducting a randomised controlled trial of a cookstove intervention in rural Malawi. *International Journal of Tuberculosis & Lung Disease*, 18(2), 240–247. <https://doi.org/10.5588/ijtld.13.0485>

Jayarathne, T., Stockwell, C. E., Bhave, P. V., Praveen, P. S., Rathnayake, C. M., Islam, M. R., et al. (2018). Nepal Ambient Monitoring and Source Testing Experiment (NAMaSTE): Emissions of particulate matter from wood- and dung-fueled cooking fires, garbage and crop residue burning, brick kilns, and other sources. *Atmospheric Chemistry and Physics*, 18(3), 2259–2286. <https://doi.org/10.5194/acp-18-2259-2018>

Jetter, J., Zhao, Y., Smith, K. R., Khan, B., Yelverton, T., Decarlo, P., & Hays, M. D. (2012). Pollutant emissions and energy efficiency under controlled conditions for household biomass cookstoves and implications for metrics useful in setting international test standards. *Environmental Science & Technology*, 46(19), 10827–10834. <https://doi.org/10.1021/es301693f>

Johnson, M., Lam, N., Pennise, D., Charron, D., Bond, T., Modi, V., & Ndemere, J. (2011). *Home emissions of greenhouse pollutants from rocket and traditional biomass cooking stoves in Uganda*: US Agency for International Development.

Johnston, F., Hanigan, I., Henderson, S., Morgan, G., & Bowman, D. (2011). Extreme air pollution events from bushfires and dust storms and their association with mortality in Sydney, Australia 1994–2007. *Environmental Research*, 111(6), 811–816. <https://doi.org/10.1016/j.envres.2011.05.007>

Johnston, F. H., Henderson, S. B., Chen, Y., Randerson, J. T., Marlier, M., DeFries, R. S., et al. (2012). Estimated global mortality attributable to smoke from landscape fires. *Environmental Health Perspectives*, 120(5), 695–701. <https://doi.org/10.1289/ehp.1104422>

Kim, Y. H., Warren, S. H., Krantz, Q. T., King, C., Jaskot, R., Preston, W. T., et al. (2018). Mutagenicity and lung toxicity of smoldering vs flaming emissions from various biomass fuels: Implications for health effects from wildland fires. *Environmental Health Perspectives*, 126(1), 017011. <https://doi.org/10.1289/EHP2200>

Klimont, Z., Cofala, J., Xing, J., Wei, W., Zhang, C., Wang, S., et al. (2009). Projections of SO_2 , NO_x and carbonaceous aerosols emissions in Asia. *Tellus B: Chemical and Physical Meteorology*, 61(4), 602–617. <https://doi.org/10.1111/j.1600-0889.2009.00428.x>

Klimont, Z., Smith, S. J., & Cofala, J. (2013). The last decade of global anthropogenic sulfur dioxide: 2000–2011 emissions. *Environmental Research Letters*, 8(1), 014003. <https://doi.org/10.1088/1748-9326/8/1/014003>

Lamarque, J. F., Bond, T. C., Eyring, V., Granier, C., Heil, A., Klimont, Z., et al. (2010). Historical (1850–2000) gridded anthropogenic and biomass burning emissions of reactive gases and aerosols: Methodology and application. *Atmospheric Chemistry and Physics*, 10(15), 7017–7039. <https://doi.org/10.5194/acp-10-7017-2010>

Lim, C. Y., Hagan, D. H., Coggan, M. M., Koss, A. R., Sekimoto, K., de Gouw, J., et al. (2019). Secondary organic aerosol formation from the laboratory oxidation of biomass burning emissions. *Atmospheric Chemistry and Physics*, 19(19), 12797–12809. <https://doi.org/10.5194/acp-19-12797-2019>

Liousse, C., Assamoi, E., Criqui, P., Granier, C., & Rosset, R. (2014). Explosive growth in African combustion emissions from 2005 to 2030. *Environmental Research Letters*, 9, 035003. <https://doi.org/10.1088/1748-9326/9/3/035003>

Liousse, C., Guillaume, B., Grégoire, J. M., Mallet, M., Galy, C., Pont, V., et al. (2010). Updated African biomass burning emission inventories in the framework of the AMMA-IDAF program, with an evaluation of combustion aerosols. *Atmospheric Chemistry and Physics*, 10(19), 9631–9646. <https://doi.org/10.5194/acp-10-9631-2010>

Liu, X., Huey, L. G., Yokelson, R. J., Selimovic, V., Simpson, I. J., Müller, M., et al. (2017). Airborne measurements of western U.S. wildfire emissions: Comparison with prescribed burning and air quality implications. *Journal of Geophysical Research: Atmospheres*, 122(11), 6108–6129. <https://doi.org/10.1002/2016jd026315>

MacCarty, N., Still, D., & Ogle, D. (2010). Fuel use and emissions performance of fifty cooking stoves in the laboratory and related benchmarks of performance. *Energy for Sustainable Development*, 14(3), 161–171. <https://doi.org/10.1016/j.esd.2010.06.002>

Maricq, M. M., & Xu, N. (2004). The effective density and fractal dimension of soot particles from premixed flames and motor vehicle exhaust. *Journal of Aerosol Science*, 35(10), 1251–1274. <https://doi.org/10.1016/j.jaerosci.2004.05.002>

May, A. A., McMeeking, G. R., Lee, T., Taylor, J. W., Craven, J. S., Burling, I., et al. (2014). Aerosol emissions from prescribed fires in the United States: A synthesis of laboratory and aircraft measurements. *Journal of Geophysical Research: Atmospheres*, 119(2011), 11826–11849. <https://doi.org/10.1002/2014jd021848>

McClure, C. D., & Jaffe, D. A. (2018). Investigation of high ozone events due to wildfire smoke in an urban area. *Atmospheric Environment*, 194, 146–157. <https://doi.org/10.1016/j.atmosenv.2018.09.021>

McClure, C. D., Lim, C. Y., Hagan, D. H., Kroll, J. H., & Cappa, C. D. (2020). Biomass-burning-derived particles from a wide variety of fuels – Part 1: Properties of primary particles. *Atmospheric Chemistry and Physics*, 20(3), 1531–1547. <https://doi.org/10.5194/acp-20-1531-2020>

McMeeking, G. R., Kreidenweis, S. M., Baker, S., Carrico, C. M., Chow, J. C., Collett, J. L., et al. (2009). Emissions of trace gases and aerosols during the open combustion of biomass in the laboratory. *Journal of Geophysical Research*, 114(D19), D19210. <https://doi.org/10.1029/2009jd011836>

McMurry, P. H., Wang, X., Park, K., & Ebara, K. (2002). The relationship between mass and mobility for atmospheric particles: A new technique for measuring particle density. *Aerosol Science and Technology*, 36(2), 227–238. <https://doi.org/10.1080/027868202753504083>

Mitchell, E. J. S., Ting, Y., Allan, J., Lea-Langton, A. R., Spracklen, D. V., McFiggans, G., et al. (2019). Pollutant emissions from improved cookstoves of the type used in Sub-Saharan Africa. *Combustion Science and Technology*, 192(8), 1582–1602. <https://doi.org/10.1080/00102202.2019.1614922>

Mutlu, E., Warren, S. H., Ebersviller, S. M., Kooter, I. M., Schmid, J. E., Dye, J. A., et al. (2016). Mutagenicity and Pollutant emission factors of solid-fuel cookstoves: Comparison with other combustion sources. *Environmental Health Perspectives*, 124(7), 974–982. <https://doi.org/10.1289/ehp.1509852>

Naeher, L. P., Brauer, M., Lipsett, M., Zelikoff, J. T., Simpson, C. D., Koenig, J. Q., & Smith, K. R. (2007). Woodsmoke health effects: A review. *Inhalation Toxicology*, 19(1), 67–106. <https://doi.org/10.1080/08958370600985875>

Ng, N. L., Herndon, S. C., Trimborn, A., Canagaratna, M. R., Croteau, P. L., Onasch, T. B., et al. (2011). An aerosol chemical speciation monitor (ACSM) for routine monitoring of the composition and mass concentrations of ambient aerosol. *Aerosol Science and Technology*, 45(7), 780–794. <https://doi.org/10.1080/02786826.2011.560211>

Oluwole, O., Ana, G. R., Arinola, G. O., Wiskel, T., Falusi, A. G., Huo, D., et al. (2013). Effect of stove intervention on household air pollution and the respiratory health of women and children in rural Nigeria. *Air Quality, Atmosphere & Health*, 6(3), 553–561. <https://doi.org/10.1007/s11869-013-0196-9>

Pandey, A., Patel, S., Pervez, S., Tiwari, S., Yadama, G., Chow, J. C., et al. (2017). Aerosol emissions factors from traditional biomass cookstoves in India: Insights from field measurements. *Atmospheric Chemistry and Physics*, 17(22), 13721–13729. <https://doi.org/10.5194/acp-17-13721-2017>

Park, K., Cao, F., Kittelson, D. B., & McMurry, P. H. (2003). Relationship between particle mass and mobility for diesel exhaust particles. *Environmental Science & Technology*, 37(3), 577–583. <https://doi.org/10.1021/es025960v>

Park, K., Kittelson, D. B., & McMurry, P. H. (2004). Structural properties of diesel exhaust particles measured by transmission electron microscopy (TEM): Relationships to particle mass and mobility. *Aerosol Science and Technology*, 38(9), 881–889. <https://doi.org/10.1080/02786829050189>

Pennise, D., Brant, S., Agbeve, S. M., Quaye, W., Mengesha, F., Tadele, W., & Wofchuk, T. (2009). Indoor air quality impacts of an improved wood stove in Ghana and an ethanol stove in Ethiopia. *Energy for Sustainable Development*, 13(2), 71–76. <https://doi.org/10.1016/j.esd.2009.04.003>

Permar, W., Wang, Q., Selimovic, V., Wielgazs, C., Yokelson, R. J., Hornbrook, R. S., et al. (2021). Emissions of trace organic gases from western U.S. wildfires based on WE-CAN aircraft measurements. *Journal of Geophysical Research: Atmospheres*, 126, e2020JD033838. <https://doi.org/10.1029/2020JD033838>

Pokhrel, R. P., Gordon, J., Fiddler, M. N., & Bililign, S. (2021). Impact of combustion conditions on physical and morphological properties of biomass burning aerosol. *Aerosol Science and Technology*, 55(1), 80–91. <https://doi.org/10.1080/02786826.2020.1822512>

Pokhrel, R. P., Wagner, N. L., Langridge, J. M., Lack, D. A., Jayaratne, T., Stone, E. A., et al. (2016). Parameterization of single-scattering albedo (SSA) and absorption Ångström exponent (AAE) with EC/OC for aerosol emissions from biomass burning. *Atmospheric Chemistry and Physics*, 16(15), 9549–9561. <https://doi.org/10.5194/acp-16-9549-2016>

Rappold, A. G., Stone, S. L., Cascio, W. E., Neas, L. M., Kilaru, V. J., Carraway, M. S., et al. (2011). Peat bog wildfire smoke exposure in rural North Carolina Is Associated with cardiopulmonary emergency department visits assessed through syndromic surveillance, *Environmental Health Perspectives*, 119(10), 1415–1420. <https://doi.org/10.1289/ehp.1003206>

Redemann, J., Wood, R., Zuidema, P., Doherty, S. J., Luna, B., LeBlanc, S. E., et al. (2020). An overview of the ORACLES (ObserveRvations of Aerosols above CLouds and their intEractionS) project: Aerosol-cloud-radiation interactions in the Southeast Atlantic basin. *Atmospheric Chemistry and Physics*. <https://doi.org/10.5194/acp-2020-449>

Reid, J. S., Koppmann, R., Eck, T. F., & Eleuterio, D. P. (2005). A review of biomass burning emissions part II: Intensive physical properties of biomass burning particles. *Atmospheric Chemistry and Physics*, 5, 799–825. <https://doi.org/10.5194/acp-5-799-2005>

Roberts, G., Wooster, M. J., & Lagoudakis, E. (2009). Annual and diurnal African biomass burning temporal dynamics. *Biogeosciences*, 6(5), 849–866. <https://doi.org/10.5194/bg-6-849-2009>

Roberts, G. J., & Wooster, M. J. (2008). Fire detection and fire characterization over Africa using Meteosat SEVIRI. *IEEE Transactions on Geoscience and Remote Sensing*, 46(4), 1200–1218. <https://doi.org/10.1109/TGRS.2008.915751>

Roden, C. A., Bond, T. C., Conway, S., & Osorio Pinel, A. B. (2006). Emission factors and real-time optical properties of particles emitted from traditional wood burning cookstoves. *Environmental Science & Technology*, 40, 6750–6757. <https://doi.org/10.1021/es052080i>

Roden, C. A., Bond, T. C., Conway, S., Osorio Pinel, A. B., MacCarty, N., & Still, D. (2009). Laboratory and field investigations of particulate and carbon monoxide emissions from traditional and improved cookstoves. *Atmospheric Environment*, 43(6), 1170–1181. <https://doi.org/10.1016/j.atmosenv.2008.05.041>

Rosa, G., Majorin, F., Boisson, S., Barstow, C., Johnson, M., Kirby, M., et al. (2014). Assessing the impact of water filters and improved cook stoves on drinking water quality and household air pollution: A randomised controlled trial in Rwanda. *PLoS One*, 9(3), e91011. <https://doi.org/10.1371/journal.pone.0091011>

Saliba, G., Subramanian, R., Bilsback, K., L'Orange, C., Volckens, J., Johnson, M., & Robinson, A. L. (2018). Aerosol Optical properties and climate implications of emissions from traditional and improved cookstoves. *Environmental Science & Technology*, 52(22), 13647–13656. <https://doi.org/10.1021/acs.est.8b05434>

Schultz, M. G., Heil, A., Hoelzemann, J. J., Spessa, A., Thonicke, K., Goldammer, J. G., et al. (2008). Global wildland fire emissions from 1960 to 2000. *Global Biogeochemical Cycles*, 22(2), GB2002. <https://doi.org/10.1029/2007GB003031>

Selimovic, V., Yokelson, R. J., Warneke, C., Roberts, J. M., de Gouw, J., Reardon, J., & Griffith, D. W. T. (2018). Aerosol optical properties and trace gas emissions by PAX and OP-FTIR for laboratory-simulated western US wildfires during FIREX. *Atmospheric Chemistry and Physics*, 18(4), 2929–2948. <https://doi.org/10.5194/acp-18-2929-2018>

Smith, D. M., Cui, T., Fiddler, M. N., Pokhrel, R. P., Surratt, J. D., & Bililign, S. (2020). Laboratory studies of fresh and aged biomass burning aerosol emitted from east African biomass fuels – Part 2: Chemical properties and characterization. *Atmospheric Chemistry and Physics*, 20(17), 10169–10191. <https://doi.org/10.5194/acp-20-10169-2020>

Smith, D. M., Fiddler, M. N., Pokhrel, R. P., & Bililign, S. (2020). Laboratory studies of fresh and aged biomass burning aerosol emitted from east African biomass fuels – Part 1: Optical properties. *Atmospheric Chemistry and Physics*, 20(17), 10149–10168. <https://doi.org/10.5194/acp-20-10149-2020>

Smith, D. M., Fiddler, M. N., Sexton, K. G., & Bililign, S. (2019). Construction and characterization of an indoor smog chamber for measuring the optical and physicochemical properties of aging biomass burning aerosols. *Aerosol and Air Quality Research*, 19(3), 467–483. <https://doi.org/10.4209/aaqr.2018.06.0243>

Smith, K. R., & Pillarisetti, A. (2017). Household air pollution from solid cookfuels and its effects on health. In C. N. Mock, R. Nugent, O. Kobusingye, & K. R. Smith (Eds.), *Injury prevention and environmental health*. (3rd ed.) The International Bank for Reconstruction and Development/The World Bank. <https://doi.org/10.1596/978-1-4648-0522-6>

Stefanidou, M., Athanasielis, S., & Spiliopoulou, C. (2008). Health impacts of fire smoke inhalation. *Inhalation Toxicology*, 20(8), 761–766. <https://doi.org/10.1080/08958370801975311>

Stockwell, C. E., Jayarathne, T., Cochrane, M. A., Ryan, K. C., Putra, E. I., Saharjo, B. H., et al. (2016). Field measurements of trace gases and aerosols emitted by peat fires in Central Kalimantan, Indonesia, during the 2015 El Niño. *Atmospheric Chemistry and Physics*, 16(18), 11711–11732. <https://doi.org/10.5194/acp-16-11711-2016>

Stockwell, C. E., Yokelson, R. J., Kreidenweis, S. M., Robinson, A. L., DeMott, P. J., Sullivan, R. C., et al. (2014). Trace gas emissions from combustion of peat, crop residue, domestic biofuels, grasses, and other fuels: Configuration and Fourier transform infrared (FTIR) component of the fourth Fire Lab at Missoula Experiment (FLAME-4). *Atmospheric Chemistry and Physics*, 14(18), 9727–9754. <https://doi.org/10.5194/acp-14-9727-2014>

Streets, D. G., Bond, T. C., Lee, T., & Jang, C. (2004). On the future of carbonaceous aerosol emissions. *Journal of Geophysical Research*, 109(D24), D24212. <https://doi.org/10.1029/2004JD004902>

Sutherland, E. R., Make, B. J., Vedral, S., Zhang, L., Dutton, S. J., Murphy, J. R., & Silkoff, P. E. (2005). Wildfire smoke and respiratory symptoms in patients with chronic obstructive pulmonary disease. *Journal of Allergy and Clinical Immunology*, 115(2), 420–422. <https://doi.org/10.1016/j.jaci.2004.11.030>

Thomas, E., Wickramasinghe, K., Mendis, S., Roberts, N., & Foster, C. (2015). Improved stove interventions to reduce household air pollution in low and middle income countries: A descriptive systematic review. *BMC Public Health*, 15, 650. <https://doi.org/10.1186/s12889-015-2024-7>

Tihay-Felicelli, V., Santoni, P. A., Gerandi, G., & Barboni, T. (2017). Smoke emissions due to burning of green waste in the Mediterranean area: Influence of fuel moisture content and fuel mass. *Atmospheric Environment*, 159, 92–106. <https://doi.org/10.1016/j.atmosenv.2017.04.002>

UN United Nations. (2017). World population prospects: The 2017 revision, key findings and advance tables. Department of Economic and Social Affairs, Population Division. Working Paper No. ESA/P/WP/248.

Vakkari, V., Kerminen, V. M., Beukes, J. P., Tiitta, P., Zyl, P. G., Josipovic, M., et al. (2014). Rapid changes in biomass burning aerosols by atmospheric oxidation. *Geophysical Research Letters*, 41(7), 2644–2651. <https://doi.org/10.1002/2014gl059396>

van der Werf, G. R., Randerson, J. T., Giglio, L., Collatz, G. J., Mu, M., Kasibhatla, P. S., et al. (2010). Global fire emissions and the contribution of deforestation, savanna, forest, agricultural, and peat fires (1997–2009). *Atmospheric Chemistry and Physics*, 10(23), 11707–11735. <https://doi.org/10.5194/acp-10-11707-2010>

Wathore, R., Mortimer, K., & Grieshop, A. P. (2017). In-use emissions and estimated impacts of traditional, natural- and forced-draft cookstoves in rural Malawi. *Environmental Science & Technology*, 51(3), 1929–1938. <https://doi.org/10.1021/acs.est.6b05557>

Yokelson, R. J., Burling, I. R., Gilman, J. B., Warneke, C., Stockwell, C. E., de Gouw, J., et al. (2013). Coupling field and laboratory measurements to estimate the emission factors of identified and unidentified trace gases for prescribed fires. *Atmospheric Chemistry and Physics*, 13(1), 89–116. <https://doi.org/10.5194/acp-13-89-2013>

Yokelson, R. J., Christian, T. J., Karl, T. G., & Guenther, A. (2008). The tropical forest and fire emissions experiment: Laboratory fire measurements and synthesis of campaign data. *Atmospheric Chemistry and Physics*, 8(13), 3509–3527. <https://doi.org/10.5194/acp-8-3509-2008>

Yokelson, R. J., Crounse, J. D., DeCarlo, P. F., Karl, T., Urbanski, S., Atlas, E., et al. (2009). Emissions from biomass burning in the Yucatan. *Atmospheric Chemistry and Physics*, 9, 5785–5812. <https://doi.org/10.5194/acp-9-5788-200910.5194/acp-9-5785-2009>

Yokelson, R. J., Goode, J. G., Ward, D. E., Susott, R. A., Babbitt, R. E., Wade, D. D., et al. (1999). Emissions of formaldehyde, acetic acid, methanol, and other trace gases from biomass fires in North Carolina measured by airborne Fourier transform infrared spectroscopy. *Journal of Geophysical Research: Atmospheres*, 104(D23), 30109–30125. <https://doi.org/10.1029/1999JD900817>

Yokelson, R. J., Susott, R. A., Ward, D. E., Reardon, J., & Griffith, D. W. T. (1997). Emissions from smoldering combustion of biomass measured by open-path Fourier transform infrared spectroscopy. *Journal of Geophysical Research*, 102(D15), 18865–18877. <https://doi.org/10.1029/97jd00852>

Reference From the Supporting Information

Simmons, W. W. (1983). *Analysis of single particle wood combustion in convective flow*. University of Wisconsin.